Verdoheme Reactivity. Remarkable Paramagnetically Shifted ^{1}H NMR Spectra of Intermediates from the Addition of Hydroxide or Methoxide with Fe^{II} and Fe^{III} Verdohemes

Lechosław Latos-Grażyński,*,‡ Jacek Wojaczyński,‡ Richard Koerner,† James J. Johnson,† and Alan L. Balch*,†

Department of Chemistry, University of California, Davis, California 95616, and Department of Chemistry, University of Wrocław, Wrocław, Poland

Received February 27, 2001

Studies of the reaction of 5-oxaporphyrin iron complexes (verdohemes) with methoxide ion or hydroxide ion have been undertaken to understand the initial step of ring opening of verdohemes. High-spin {$ClFe^{III}$(OEOP)} undergoes a complex series of reactions upon treatment with hydroxide ion in chloroform, and similar species are also detected in dichloromethane, acetonitrile, and dimethyl sulfoxide. Three distinct paramagnetic intermediates have been identified by ^{1}H NMR spectroscopy. These reactive species are formed by addition of hydroxide to the macrocycle and to the iron as an axial ligand. Treatment of low-spin [$(py)_2Fe^{II}$(OEOP)]Cl (OEOP is the monoanion of octaethyl-5-oxaporphyrin) with excess methoxide ion in pyridine solution produces {$(py)_nFe^{II}$(OEBOMe)} (n = 1 or 2) ((OEBOMe), dianion of octaethylmethoxybiliverdin), whose ^{1}H NMR spectrum undergoes marked alteration upon addition of further ammounts of methoxide ion. An identical ^{1}H NMR spectrum, which is characterized by methylene resonances with both upfield and downfield paramagnetic shifts, is formed upon treatment of {Fe^{II}(OEBOMe)}$_2$ with methoxide in pyridine solution and results from the formation of [(MeO)Fe^{II}(OEBOMe)]$^-$.

Introduction

Verdoheme is the green iron complex of the 5-oxaporphyrin macrocycle (see Scheme 1).[1−3] This green pigment can be obtained by the oxidation of an iron porphyrin by dioxygen in the presence of an excess of an axial ligand (pyridine or cyanide ion) and a reducing agent (ascorbic acid or hydrazine).[4,5] That process is known as coupled oxidation and has been used to demonstrate heme degradation for over seventy years.[6] Verdoheme can also be prepared by the cyclization and dehydration of the linear tetrapyrrole biliverdin in the presence of iron salts.[7,8] Verdohemes are spectroscopically detectable intermediates in the process of heme degradation catalyzed by heme oxygenase.[9−11] This enzyme acts on heme, as a substrate, and oxidizes it to produce biliverdin, free iron ion, and carbon monoxide in a process that involves the activation of three molecules of dioxygen.[12−14]

Scheme 1

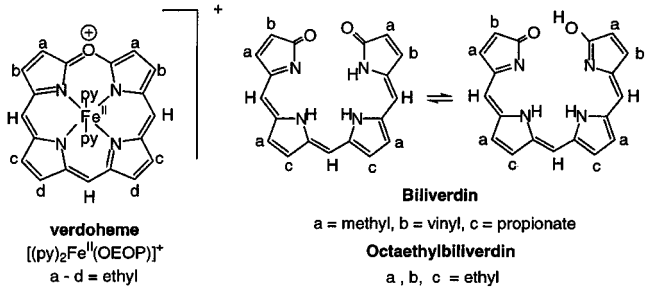

The mechanism that converts verdoheme into biliverdin and releases this linear tetrapyrrole from the enzyme is the subject of some controversy. As seen in Scheme 2, two paths for the conversion of verdohemes into biliverdin have been proposed. One (labeled A) involves hydrolysis of the 5-oxaporphyrin macrocycle; while the other (B) utilizes oxidation of the verdoheme.[15−17] The oxidative path results in release of the oxidized iron ion. Although H_3OEB **1** can undergo a two-electron oxidation,[18] it is not oxidized further in the coupled oxidation process. Heme oxygenase also apparently releases biliverdin, not its oxidation product.

* To whom correspondence should be addressed.
† University of California.
‡ University of Wrocław.

(1) Balch, A. L.; Latos-Grażyński, L.; Noll, B. C.; Olmstead, M. M.; Szterenberg, L.; Safari, N. *J. Am. Chem. Soc.* **1993**, *115*, 1422, and references therein.
(2) Balch, A. L.; Koerner, R.; Olmstead, M. M. *J. Chem. Soc., Chem. Commun.* **1995**, 873.
(3) Lagarias, J. C. *Biochim. Biophys. Acta* **1982**, *717*, 12.
(4) Balch, A. L.; Latos-Grażyński, L.; Noll, B. C.; Olmstead, M. M.; Safari, N. *J. Am. Chem. Soc.* **1993**, *115*, 9056, and references therein.
(5) Balch, A. L.; Koerner, R.; Latos-Grażyński, L.; Lewis, J. E.; St. Claire, T. N.; Zovinka, E. P. *Inorg. Chem.* **1997**, *36*, 3892.
(6) Warburg, O.; Negelein, E. *Chem. Ber.* **1930**, *63*, 1816.
(7) Saito, S.; Itano, H. A. *J. Chem. Soc., Perkin Trans.* **1986**, *1*, 1.
(8) Saito, S.; Sumita, S.; Iwai, K.; Sano, H. *Bull. Chem. Soc. Jpn.* **1988**, *61*, 3539.
(9) Wilks, A.; Ortiz de Montellano, P. R. *J. Biol. Chem.* **1993**, *268*, 22357.
(10) Takahashi, S.; Matera, K. M.; Fujii, H.; Zhou, H.; Ishikawa, K.; Yoshida, T.; Ikeda-Saito, M.; Rousseau, D. L. *Biochemistry* **1997**, *36*, 1402.
(11) Liu, Y.; Moënne-Loccoz, P.; Leohr, T. M.; Ortiz de Montellano, P. R. *J. Biol. Chem.* **1997**, *272*, 6909.
(12) Maines, M. D. *Heme Oxygenase: Clinical Applications and Functions*; CRC Press: Boca Raton, FL, 1992.
(13) Ortiz de Montellano; P. R., *Acc. Chem. Res.* **1998**, *31*, 543.
(14) Yoshida, T.; Migita, C. T. *J. Inorg. Biochem.* **2000**, *82*, 33.
(15) Hirota, T.; Itano, H. A. *Tetrahedron Lett.* **1983**, *24*, 995.
(16) Sano, S.; Sano, T.; Morishima, I.; Shiro, Y.; Maeda, Y. *Proc. Natl. Acad. Sci. U.S.A.* **1986**, *83*, 531.
(17) Saito, S.; Itano, H. A. *Proc. Natl. Acad. Sci. U.S.A.* **1982**, *79*, 1393.
(18) Balch, A. L.; Koerner, R.; Olmstead, M. M.; Safari, N.; St. Claire, T. *J. Chem. Soc., Chem. Commun.* **1995**, 643.

10.1021/ic010227a CCC: $20.00
Published on Web 08/09/2001

Scheme 2

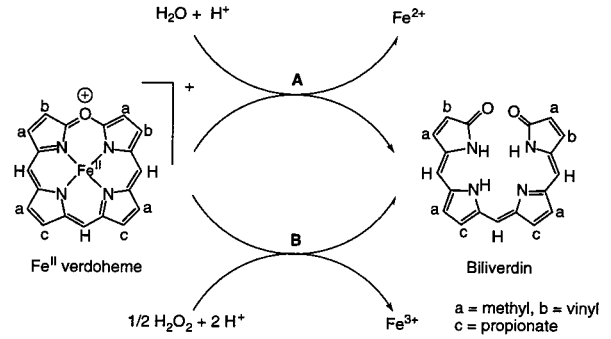

Scheme 3

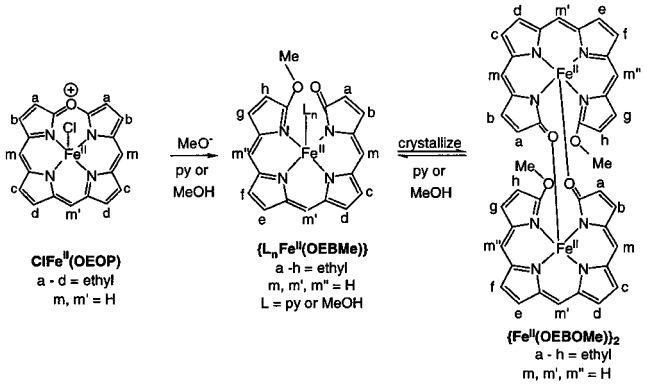

The hydrolytic pathway is generally considered to begin with addition of hydroxide to verdoheme. Consequently, this laboratory has been examining the reactivity of verdoheme and related complexes with a variety of nucleophiles. For example, addition of methoxide to $ClFe^{II}$(OEOP) causes ring opening as shown in Scheme 3, and the dimeric complex $\{Fe^{II}(OEBOMe)\}_2$ has been isolated in crystalline form from this reaction.[19] Methoxide, rather that hydroxide, was used in that study so further deprotonation/protonation reactions that might follow the initial attack were avoided. Additionally, ring-opened products resulting from the addition of alkoxide, thiolate, and amide ions to zinc verdoheme were isolated and crystallographically characterized.[20,21]

Results

Method of Spectral Analysis. To simplify the description and identification of individual species responsible for the ^{1}H NMR spectra, we will refer to the particular spectroscopic pattern as $\{m/n/l\}$, where m, n, and l are the number of meso, methyl, and methylene resonances for any one species. Thus for $ClFe^{II}$(OEOP), the spectrum is expected to be of the $\{2/4/8\}$ type, with two meso resonances (intensity ratio 2:1), four methyl resonances, and eight methylene resonances.[1] For L_nFe^{II}(OEBOMe), the spectrum should be of the $\{3/8/16\}$ type, with three meso resonances, eight methyl resonances, and sixteen methylene resonances.[19] If a difference in the signs of the chemical shifts is observed for a particular functional group, the division into two subsets is also indicated as e.g. $\{m/n/(l_1^+ + l_2^-)\}$, where l_1^+ is the number of methylene resonances shifted downfield and l_2^- is the number of methylene resonances shifted upfield. For the ring opening products generated from X_2Fe^{III}(OEOP),[1] a ^{1}H NMR spectrum of the $\{3/8/16\}$ type is expected if the product is helical and the axial ligands are different or if the substitution at the terminal C(1) and C(19) carbon atoms is different (e.g., O and OH, or O and OMe). If the symmetry of the helical complex increases because the axial ligands are identical or the two terminal substituents are identical, the spectrum will simplify to $\{2/4/8\}$ with two meso resonances (intensity ratio 2:1), four methyl resonances, and eight methylene resonances, as seen for instance for (OEB)-Cu[22] and $(OEB)Fe^{III}(py)_2$.[4]

Consequently, in our NMR analysis we have considered these $\{3/8/16\}$ patterns or their variations as "fingerprints" of an individual iron biliverdin complex. Since the relative intensities of resonances assigned to a single species remain constant, but resonances related to different forms can vary in intensity, we could identify the majority of resonances generated by a single form, even in a complex mixture of compounds.

As usual for complexes derived from octaethylporphyrin, the meso resonances are expected to be broader than the methylene or methyl resonances of the ethyl groups due to the closer proximity of the meso groups to the paramagnetic center. Consequently, these meso resonances are generally expected to be the broadest resonances in the ^{1}H NMR spectrum as a result of metal ion centered dipolar relaxation.[23] However, the effects related to scalar relaxation and dipolar relaxation by delocalized spin density (ρ_C) on aromatic carbon atoms also influence the line widths.[24,25] Both scalar relaxation and dipolar relaxation are proportional to $(\rho_C)^2$. Accordingly, a linear relationship between the line widths and $(\rho_C)^2$ is theoretically expected. Qualitatively, we have determined a strong dependence of the meso line widths on the absolute value of the contact shifts, particularly in spectra of the radical-like species (vide infra in Figures 3 and 8). These meso resonances may also be easily identified in the ^{1}H NMR spectra collected under inversion recovery conditions providing that the delay time τ has been chosen in such a way that only resonances with relatively short relaxation times can be detected. To support the assignment of meso resonances, parallel experiments with the addition of KOD/D_2O to (OEOP-*meso*-d_3)$Fe^{III}Cl_2$ have also been carried out.

Hydroxide Addition to Cl_2Fe^{III}(OEOP). Addition of potassium hydroxide (1 M solution in D_2O) to a 2 mM dichloromethane-d_2 solution of Cl_2Fe^{II}(OEOP) **2** produces marked changes in the ^{1}H NMR spectra of the sample, as seen in Figure 1. Trace A shows the ^{1}H NMR spectrum of Cl_2Fe^{II}(OEOP) before the addition of potassium hydroxide. As reported previously,[1] this spectrum belongs the $\{2/4/4\}$ type. Addition of 4 μL of the potassium hydroxide solution to the Cl_2Fe^{II}(OEOP) sample produces the spectrum shown in Trace B. The resonances of Cl_2Fe^{II}(OEOP) have decreased in intensity, and two new sets of resonances assigned to two different intermediates, **3** and **4**, have grown in intensity. These resonances are easily differentiated in the upfield region, where they are labeled **3** and **4**, but overlap with resonances of each other and of the starting material

(19) Koerner, R.; Latos-Grażyński, L.; Balch, A. L. *J. Am. Chem. Soc.* **1998**, *120*, 9246.
(20) Latos-Grażyński, L.; Johnson, J. J.; Attar, S.; Olmstead, M. M.; Balch, A. L. *Inorg. Chem.* **1998**, *37*, 4493.
(21) Johnson, J. J.; Olmstead, M. M.; Balch, A. L. *Inorg. Chem.* **1999**, *38*, 5379
(22) Balch, A. L.; Mazzanti, M.; Noll, B. C.; Olmstead, M. M. *J. Am. Chem. Soc.* **1993**, *115*, 12206.
(23) Balch, A. L.; Latos-Grażyński, L.; Noll, B. C.; Olmstead, M. M.; Zovinka, E. P. *Inorg. Chem.* **1992**, *31*, 2248.
(24) Walker, F. A. Proton NMR Spectroscopy of Paramagnetic Metalloporphyrins. In *The Porphyrin Handbook*; Kadish, K. M., Smith, K. M., Guilard, R., Eds.; Academic Press: New York, 2000; Vol. 5, p 81 (see p 92).
(25) Unger, S. W.; Jue, T.; La Mar, G. N. *J. Magn. Res.* **1985**, *61*, 448.

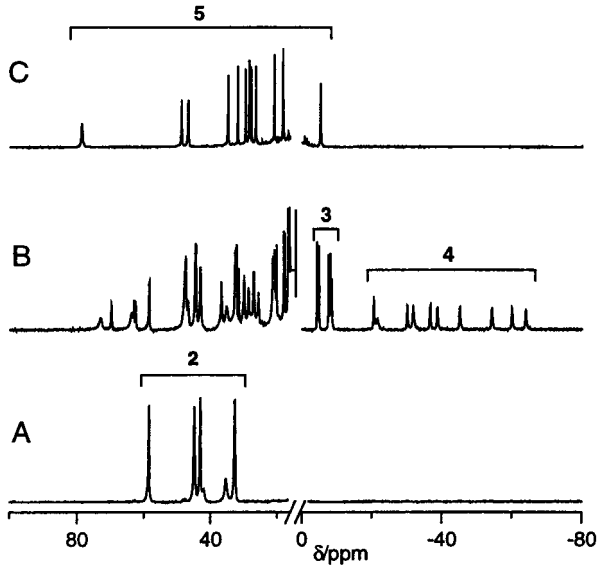

Figure 1. ^{1}H NMR spectra at 500 MHz resulting from titration of a solution of Cl_2Fe^{III}(OEOP) (**2**), in dichloromethane-d_2, with a 1.0 M solution of KOD, in D_2O at 297 K. Trace A shows the initial spectrum of Cl_2Fe^{III}(OEOP) (**2**). Traces B and C show the effects of additions of 4 μL (B) and 10 μL (C) of the KOD solution to the original sample. For clarity the 0−15 ppm regions of all spectra are omitted. Diagnostic signals of **2**, and intermediates **3**, **4**, and **5** are indicated in the spectra.

in the downfield region. Addition of a further 6 μL of titrant produces the spectrum shown in Trace C. At this point, all of the resonances of intermediates **3** and **4**−Cl as well as those of Cl_2Fe^{II}(OEOP) have diminished to the point where they are no longer observed, but the resonances of a new intermediate **5** have grown.

Spectral changes similar to those seen in Figure 1 are also observed when a potassium hydroxide solution is added to a solution of Cl_2Fe^{II}(OEOP) in other solvents including chloroform-*d*, acetonitrile-d_3, and dimethyl sulfoxide-d_6. Consequently, the spectral changes seen in Figure 1 cannot be specifically ascribed to reactions of the solvent with Cl_2Fe^{II}(OEOP), but must arise from addition of hydroxide to the complex.

A spectral range from 90 to −80 ppm has been arbitrarily used to create Figure 1. However, some of the intermediates that form exhibit resonances with even larger paramagnetic shifts that are well outside the spectral window used to generate Figure 1. Consequently, the spectra of these intermediates have been examined further under conditions where the relative amount of each intermediate has been optimized by carefully adjusting the quantity of potassium hydroxide added.

Figure 2 shows the spectrum of a sample that contains predominantly intermediate **3**. However, the spectrum of this intermediate is accompanied by resonances of intermediate **4**−Cl as well as resonances originating with an additional, unidentified species. The methylene resonances of **3** reveal an alternation of the sign of the paramagnetic shifts. Nine methylene resonances can be identified in the downfield region (8.6, 9.3, 10.5, 11.2, 12.5, 12.9, 13.9, 14.3, and 16.4 ppm) while five (0.2, −8.2, −8.6, −11.5, and −11.5 ppm at 297 K) are observed in the upfield region. The observation of this number of methylene resonances suggests that we are dealing with a spectrum of the {3/8/16} type. However, only one out of the expected three meso resonances for **3** has been detected at −12.4 ppm, and the remaining meso and methylene resonances are likely to be in regions where they overlap other resonances.

Intermediate **4**−Cl can be obtained in essentially pure form by carefully conducting the addition of the potassium hydroxide

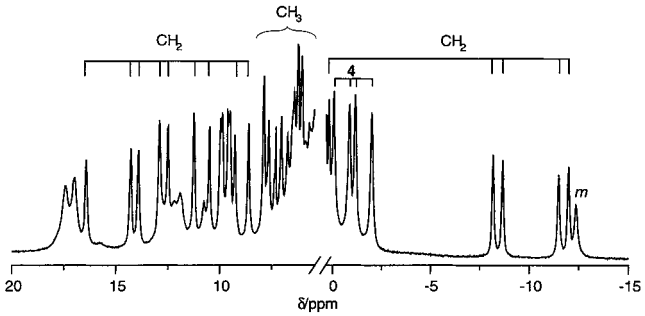

Figure 2. 500 MHz ^{1}H NMR spectrum of intermediate **3** in dichloromethane-d_2 at 297 K. Methyl, methylene, and meso resonances are labeled CH_3, CH_2, and m, respectively. Methyl resonances of compound **4**−Cl are also indicated in the −3 to 0 ppm region. The crowded 0.5−5.5 ppm part of the spectrum is not shown.

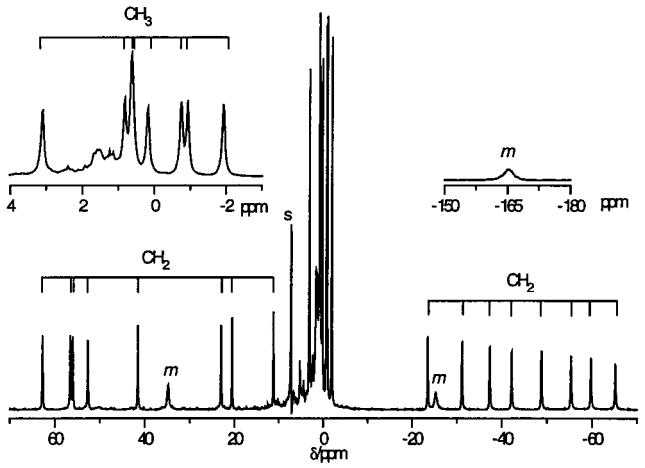

Figure 3. 500 MHz ^{1}H NMR spectrum of **4**−Cl in chloroform-*d* at 303 K. Insets present methyl peaks in the −3 to 4 ppm region and the most upfield shifted meso resonance. Resonance labeling follows that of Figure 2.

solution in chloroform-*d*. The spectrum of intermediate **4**−Cl is shown in Figure 3. In this case, all resonances of the intermediate have been identified. Eight methylene resonances are spread out in the low field region from 10 to 65 ppm with chemical shifts (measured at 303 K) of 11.2 ($\Delta\nu_{1/2} = 55$), 20.6 (52), 23.0 (58), 41.6 (57), 52.7 (72), 56.0 (67), 56.5 (65), and 62.7 ppm (65 Hz). Eight other methylene resonances occur in the high field region from −20 to −70 ppm with chemical shifts of −23.5 (66), −31.1 (71), −37.3 (75), −42.1 (83), −48.8 (81), −55.3 (89), −59.8 (93), and −65.2 ppm (104 Hz). Eight methyl resonances are located in the −2 to 3 ppm region. Finally, two meso resonances are shifted upfield to −25.2 ($\Delta\nu_{1/2} = 320$) and −165.2 ppm (600 Hz), and the third one is located in the downfield region at 34.9 ppm (220 Hz).

The line widths of the methylene and methyl resonances of intermediate **4**−Cl are relatively narrow. Consequently, a two-dimensional MCOSY spectrum has been used to identify protons within individual ethyl groups. Figure 4 shows the MCOSY map obtained for **4**−Cl in chloroform-*d* at 303 K. Cross-peaks reveal pairwise coupling between the sixteen methylene resonances, and further cross-peaks connect these pairs with the eight methyl resonances. The results of these assignments were used to identify the resonances in Figure 3. Note that no cross-peaks are observed for the resonances assigned to the meso protons as a result of the broadness of these resonances and their isolation from other spins.

The resonances of intermediate **4** are sensitive to the anionic axial ligands that may be present. As seen in Figure 5, addition

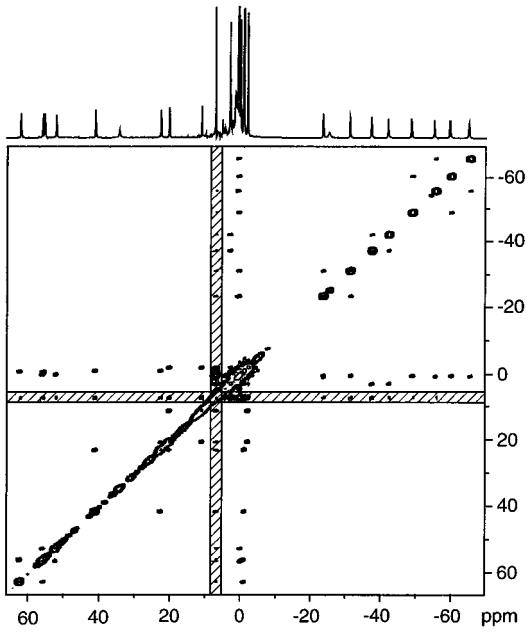

Figure 4. 500 MHz MCOSY map for compound **4**−Cl in chloroform-*d* at 303 K. The shaded part of spectrum consists of artifacts due to the strong solvent resonance.

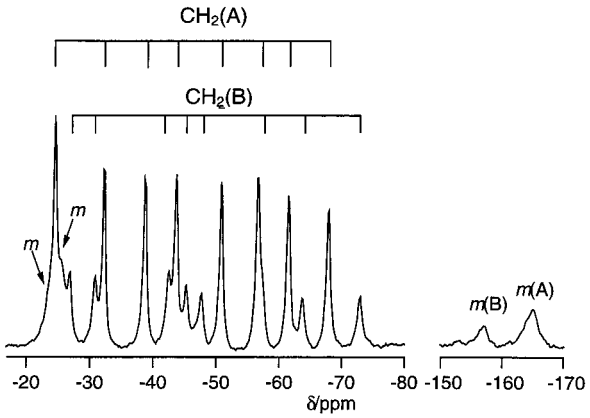

Figure 5. An upfield portion of the 300 MHz ^{1}H NMR spectrum of the solution containing the **4**−Cl (A) and **4**−TFA (B) formed by adding HTFA to the sample of **4**−Cl in chloroform-*d* solution at 293 K.

of trifluoroacetic acid (HTFA) to a solution of **4**−Cl produces spectral changes which result in development of a new set of resonances which have only small chemical shift changes relative to those of **4**−Cl. The new resonances are ascribed to another intermediate, **4**-TFA, with the trifluoroacetate (TFA) (or possibly water) acting as an axial ligand. Figure 5 shows the resonances in the upfield region only, but similar new resonances are also seen in the downfield region. In this experiment we are adding the trifluoroacetic acid to a solution which contains a considerable amount of KOD. Thus, the neutralization process produces the respective anion which is able to carry out the axial ligand metathesis. Further evidence for variation in axial ligation comes from monitoring the addition of potassium hydroxide to Br_2Fe^{II}(OEOP) in chloroform-*d*. This titration produces intermediate **4**−Br with a spectrum similar to that shown in Figure 3 but with slightly different chemical shifts for all resonances. Intermediates **4**−Cl and **4**−Br are interconvertible. Titration of **4**−Br with HCl/$CDCl_3$ results in the gradual formation of **4**−Cl. During the titration, both species can be detected simultaneously, particularly in the upfield portion of the ^{1}H NMR spectrum: (for **4**−Br methylene, −20.4, −30.1, −37.7, −44.4, −46.8, −54.9, −55.9, −63.5; meso, −31, −145.1 ppm; for **4**−Cl methylene, −24.6, −32.4, −38.8, −43.9, −51.2, −56.8, −61.8, −68.3; meso, −25.6, −166.4 in $CDCl_3$ at 293 K).

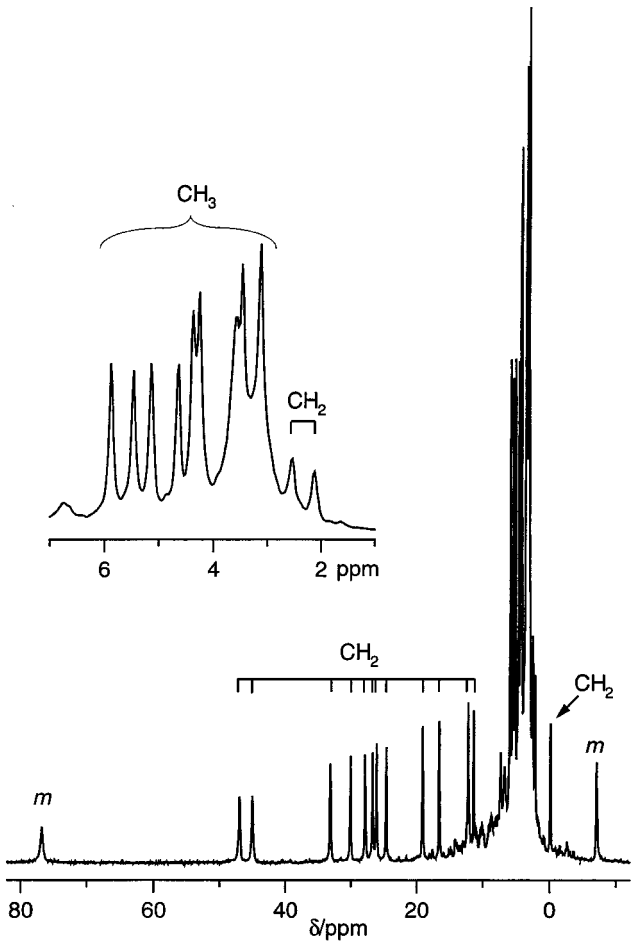

Figure 6. 500 MHz ^{1}H NMR spectrum of **5** in dichloromethane-d_2 at 297 K. The inset presents the intense signals in the 5 to −1 ppm region. The labeling follows that used in Figure 2.

Figure 6 shows the ^{1}H NMR spectrum of intermediate **5**. The assignment of the resonances of **5** is relatively straightforward. In the 9−50 ppm region, twelve of the expected sixteen methylene resonances have been detected (at 45.0, 43.0, 31.1, 28.1, 25.8, 24.7, 24.1, 22.6, 17.1, 14.6, 10.2, and 9.4 ppm), while three other methylene resonances are found at 0.6, 0.2, and −2.0 ppm. Two of the three meso resonances are found at −9.0 and 74.8 ppm (all shifts in dichloromethane-d_2, at 297 K). Unexpectedly, they reveal opposite signs of the isotropic shifts. The assignment of these two resonances has been confirmed by examining the ^{1}H NMR spectrum of intermediate **5**, which was prepared from Cl_2Fe^{II}(OEOP-*meso*-d_3). Under these conditions, the two resonances assigned to the meso protons are absent from the ^{1}H NMR spectrum. The remaining resonances of this intermediate are either hidden in the crowded region between 1 and 4 ppm or are too broad to detect. Comparison of the ^{1}H NMR spectra of samples of intermediate **5** prepared from Cl_2Fe^{II}(OEOP) and from Br_2Fe^{II}(OEOP) reveals that both spectra are identical. Thus, it is unlikely that chloride or bromide axial ligands are present in intermediate **5**. Significantly, titration of **5** with trifluoroacetic acid resulted in the generation of **4**−TFA. The observed acid−base reversibility, i.e., the conversion of **5** into **4**, is consistent with a simple coordiantion of an axial ligand accompanied by protonation of the terminal oxygen atom.

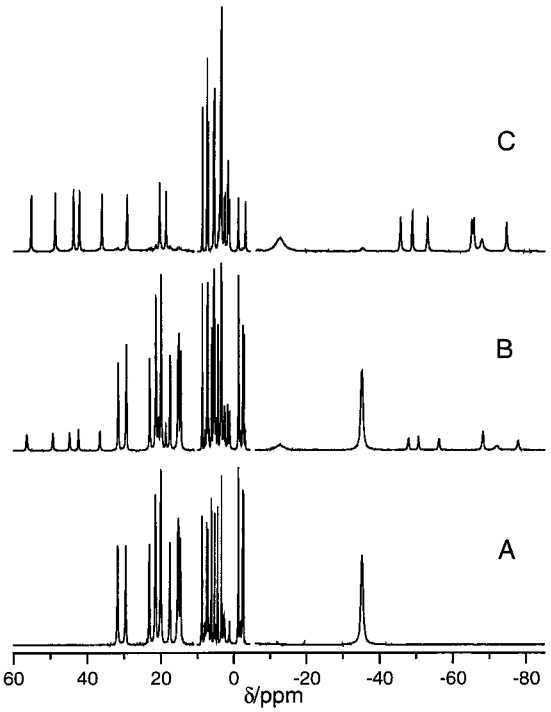

Figure 7. 500 MHz ^{1}H NMR spectra obtained by titration of $(py)_nFe^{II}$(OEBOMe) in pyridine-d_5, solution at 293 K, with a solution of KOMe in methanol−d_4. Trace A presents the spectrum for the starting compound, $(py)_nFe^{II}$(OEBOMe). Traces B and C show the effect of addition of 3 and 10 μL of KOMe solution, respectively.

In this titration, we detected one more component, the dimeric compound $\{(OEB)Fe^{III}\}_2$, although always in a rather minor concentration. A distinctive set of three meso resonances at ca. −14.4, −38.5, and −54.6 ppm occur in the upfield region, while sixteen peaks appear in the downfield region. A similar spectrum has been reported for $\{(OEB)Fe^{III}\}_2$, which was obtained as a product of the coupled oxidation of $(OEP)Fe^{II}(py)_2$ in pyridine.[4] The dimeric compound $\{(OEB)Fe^{III}\}_2$ has been identified by combination of ^{1}H NMR and X-ray crystallographic studies. In the presence of pyridine, it dissociates to form $(py)_2Fe^{III}$(OEB).[4] Under the conditions used to obtain the ^{1}H NMR spectra of the intermediates seen in Figure 1, there always is excess water and hydroxide ion present. With these axial ligands available, $\{Fe^{III}(OEB)\}_2$ does not form to a significant extent.

Methoxide Addition to $[(py)_2Fe^{II}(OEOP)]Cl$ and to $(py)_nFe^{II}$(OEBOMe). Addition of a solution of potassium hydroxide in methanol or sodium methoxide in methanol to a green, pyridine solution of diamagnetic $[(py)_2Fe^{II}(OEOP)]Cl$ in the absence of dioxygen produces a yellow−brown, air-sensitive solution that contains $(py)_nFe^{II}$(OEBOMe), as described previously.[19] The spectrum of $(py)_nFe^{II}$(OEBOMe) is shown in Trace A of Figure 7. Addition of further quantities of methoxide to $(py)_nFe^{II}$(OEBOMe) produces a significant alteration in the ^{1}H NMR spectrum. Similar spectral changes are seen when methoxide is added to a pyridine solution prepared by dissolving $\{Fe^{II}(OEBOMe)\}_2$ in pyridine-d_5. These changes are shown for the 60 to −85 ppm spectral region in Traces B and C of Figure 7. During the titration, the intensity of the spectral features due to $(py)_nFe^{II}$(OEBOMe) decline in intensity, while a new set of resonances from a single new species, which we will identify as intermediate **6**, grow. In Trace B the spectral characteristics of both species are seen, while in Trace C the conversion to the intermediate **6** is nearly complete.

In Trace C, eight methylene resonances for intermediate **6** have been detected in the downfield region with the following chemical shifts (and line widths): 18.8 ($\Delta\nu_{1/2} = 110$), 21.0 (91), 29.7 (122), 36.9 (110), 42.7 (98), 45.1 (111), 49.7 (113), and 56.7 ppm (123 Hz). Seven of the expected eight methylene resonances are observed in the upfield region as follows: −47.8 (186), −50.8 (147), −56.3 (190), −68.4 (two overlapped resonances, 193), −72.1 (485), and −77.9 ppm (217 Hz) in pyridine-d_5 solution at 293 K. In the upfield region, the variation of line widths is quite striking, and we presume that the missing eighth resonance is broadened beyond detection. The methylene resonances are accompanied by methyl resonances (−4 to 5 ppm).

A unique resonance at −12.5 ppm ($\Delta\nu_{1/2}$ = ca. 1100 Hz) with an intensity corresponding to three protons is assigned to the methoxy group of the OEBOMe ligand in intermediate **6**. This peak is absent from the spectrum when the sample is prepared from $[(OEBOMe\text{-}d_3)Fe^{II}(py\text{-}d_5)_n]$ and nonlabeled methoxide ion. Note that the methoxy resonance has undergone a downfield shift of ca. 20 ppm to −13 ppm. In a separate experiment, we found that exchange between the methoxy group in the complex and CD_3O^- in solution is rather slow. No deuterium incorporation into $(py)_nFe^{II}$(OEBOMe) to give $(py)_nFe^{II}$-(OEBOMe-d_3) is observed over 8 h for a sample in pyridine-d_5 to which a solution of CD_3O^-/CD_3OD has been added.

Finally, three meso proton resonances are observed for intermediate **6**. These resonances have remarkably large downfield shifts (128.8 ($\Delta\nu_{1/2} = 570$), 279 (970), and 549 ppm (ca. 3900 Hz). These resonances are not seen in the data shown in Figure 7, because they lie outside the spectral window used to construct this Figure. A composite spectrum showing all of the resonances for intermediate **6** is shown in Figure 8.

Of particular importance is the observation that titration of methanol-d_4 into a pyridine-d_5 solution of intermediate **6** converts it into $(py)_nFe^{II}$(OEBOMe). Consequently, it appears that intermediate **6** is $[(MeO)(py)_{n-1}Fe^{II}(OEBOMe)]^-$, which is obtained by simple substitution of a methoxide ion for a pyridine molecule as an axial ligand, as shown in Scheme 4. Attempts to isolate intermediate **6** have been thwarted by the facile interconversion of $(py)_nFe^{II}$(OEBOMe) and $[(MeO)(py)_{n-1}Fe^{II}(OEBOMe)]^-$.

To get some additional insight into the role of methoxide in the conversion of $(py)_nFe^{II}$(OEBOMe) into **6**, we carried out the analogous titration of $(py)_nFe^{II}$(OEBOMe) with KOD/D_2O. Under these conditions, a new intermediate **7**, which we formulate as $[(HO)(py)_{n-1}Fe^{II}(OEBOMe)]^-$, is observed. This intermediate displays distinctive upfield and downfield methylene resonances (at 45.0, 45.0, 43.0, 34.5, 28.6, and at −29.8, −31.7, −34.1, −38.7, −47.9, −50.0 ppm in py-d_5 at 293 K). The remaining resonances of the expected {3/8/16} pattern for this intermediate are partially covered by the dominant resonances of $(py)_nFe^{II}$(OEBOMe). Thus, the spectroscopic pattern of **7** resembles that of **6**. Significantly, the methoxy resonance of methoxybiliverdin has also been identified at −12.3 ppm. The degree of conversion in the whole titration was rather limited (ca. 10%). Addition of D_2O forces the reverse reaction; i.e., the transformation of **7** back to $(py)_nFe^{II}$(OEBOMe).

Discussion

The present study shows that the 5-oxaporphyrin macrocycle in the high-spin iron(III) verdoheme, Cl_2Fe^{III}(OEOP), undergoes addition of hydroxide to produce a series of paramagnetic complexes which are most readily detected by ^{1}H NMR spectroscopy.

To account for the observed ^{1}H NMR spectral patterns, we considered the following phenomena: opening of the 5-oxa-

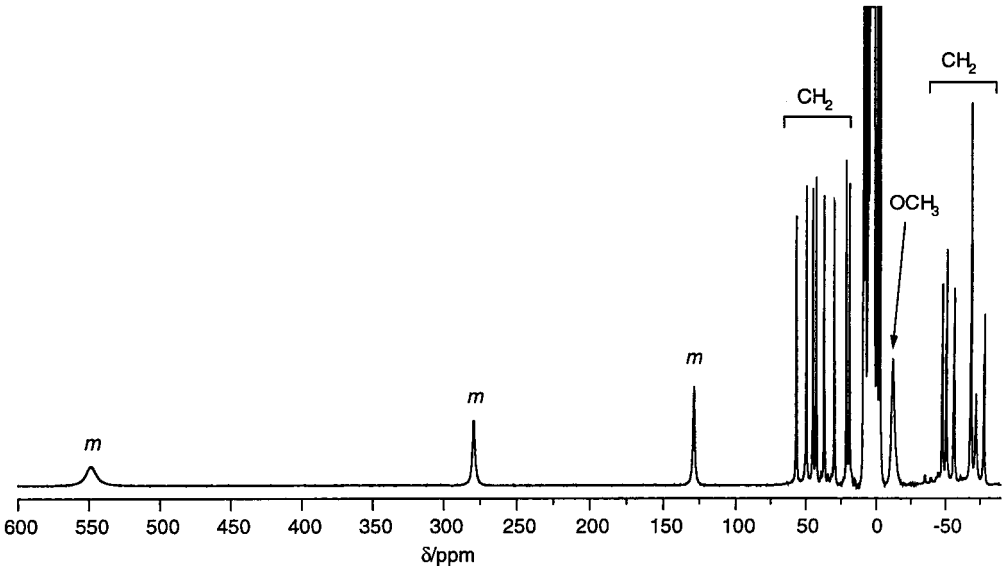

Figure 8. A composite 500 MHz ^{1}H NMR spectrum of **6** (pyridine-d_5, 293 K). Labels as in Figure 2; the methyl resonance of the methoxy group is labeled as OCH_3. This figure was composed from 5 spectra collected over the following regions: 100 to −100, 175 to −25, 100 to 300, 250 to 450, and 400 to 600 ppm. The frequency domain spectra were subsequently added to preserve the relative intensities of the resonances.

Scheme 4

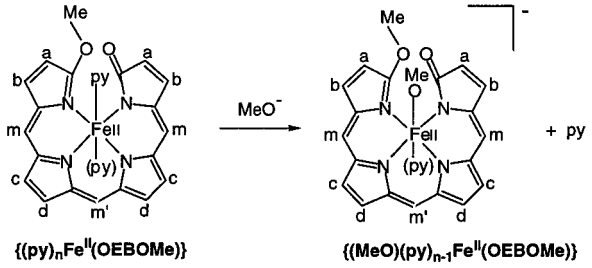

Scheme 5

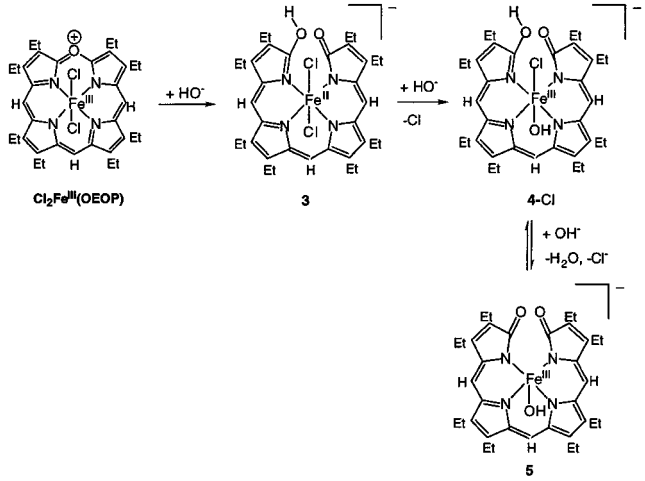

porphyrin to form biliverdin, protonation/deprotonation of the biliverdin hydroxy group, changes in coordination number of the central iron, changes of the axial ligand(s), and changes of the unpaired spin density distribution due to alteration of the axial ligation and ligand protonation. We also have considered the hypothesis that hydroxide ion might act as a reducing agent.[26] However, in our preliminary investigations, we determined that treatment of high-spin $ClFe^{II}$(OEOP) with hydroxide ion produced profound spectroscopic changes (not shown and not well understood) completely different from those observed when Cl_2Fe^{III}(OEOP) was used as the substrate. Thus, we have eliminated the possibility that some of the chemistry presented here is preceded by one-electron reduction of Cl_2Fe^{III}(OEOP) to $ClFe^{II}$(OEOP).

The process of verdoheme hydrolysis is likely to proceed as shown in Scheme 5. The partial positive charge at the 5-oxa position of the verdoheme macrocycle facilitates nucleophilic attack on the adjacent carbon to form **3**, and this is followed by the formation of **4**−Cl. This transformation to form **3** is entirely consistent with our previous observations in regard to the addition of methoxide to $ClFe^{II}$(OEOP), as shown in Scheme 3.[19] This reaction also has precedence in several examples of ring opening of zinc(II) vedohemes, where a variety of anionic nucleophiles (Nu^-) have been shown to add to $[Zn^{II}(OEOP)]^+$ to form Zn^{II}(OEBNu).[20,21] Subsequently, additional hydroxide serves to deprotonate the open chain tetrapyrrole to form intermediate **4**−Cl, which retains an axial ligand (chloride when **4**−Cl is formed from Cl_2Fe^{III}(OEOP)). Finally, addition of more hydroxide ion results in the replacement of the axial chloride ligand with a hydroxide ligand to form intermediate **5**. Intermediate **5** can undergo ligand replacement to reform **4**−X when added ligands (X^-) are present. Note that each of the intermediates shown in Scheme 5 is expected to produce an NMR spectral pattern of the {3/8/16} type. Because of the complex set of reactions that form and interconnect **3**, **4**, and **5**, it has not been possible to isolate any of these species. Nevertheless the ^{1}H NMR spectra shown in Figures 1−6 reveal the intrinsic complexity of the verdoheme hydrolysis reaction.

The ^{1}H NMR spectrum of intermediate **4**−Cl is remarkable, since the methylene and meso resonances experience both upfield and downfield hyperfine shifts in the $\{(1^+ + 2^-)/8/(8^+ + 8^-)\}$ spectroscopic pattern. This pattern is related to the electronic structure of this intermediate and reflects the unusual electronic structure of biliverdin as a ligand in the presence of oxidizible/reducible metal ions. Thus, this open chain tetrapyrrole ligand can coordinate metals ions as a diamagnetic trianion, $(OEB)^{3-}$, or as a dianionic ligand radical, $(OEB^{\bullet})^{2-}$. A number of other metal complexes of the octaethylbiliverdin ligand have been shown to possess significant ligand radical character. These include $Cu^{II}(OEB^{\bullet})$,[22] $Pd^{II}(OEB^{\bullet})$,[27] and $Ni^{II}(OEB^{\bullet})$.[27] Thus, intermediate **4**−Cl can

(26) Sawyer, D. T.; Roberts, J. L. *Acc. Chem. Res.* **1988**, *21*, 469.

be considered to involve alternative but equivalent electronic structures: $[ClFe^{III}(OEB)]^-$, with the iron as Fe(III) and the tetrapyrrole as the trianion, or as $[ClFe^{II}(OEB^{\bullet})]^-$, with Fe(II) and the ligand in a radical dianion form. These forms differ simply in the fashion in which the electrons are apportioned between the ligand and the metal. The unusual ^{1}H NMR spectral pattern seen for **4**−Cl is associated with the presence of a significant degree of ligand radical character. Two other iron complexes, $ClFe^{III}(OEPO^{\bullet})$/$ClFe^{IV}(OEPO)$[1] and $(py)_2Fe^{II}(OEPO^{\bullet})$/$(py)_2Fe^{III}(OEPO)$,[28−30] where $(OEPO^{\bullet})^{2-}$ is the dianion radical of octaethyloxophlorin and $(OEPO)^{3-}$ is the trianion of octaethyloxophlorin, also show a pattern of methylene resonances with both upfield and downfield hyperfine shifts. In considering the remarkable methylene resonance pattern with both upfield and downfield hyperfine shifts for **4**−Cl, it is important to note that the thorough resonance assignments obtained for $(py)_2Fe^{II}(OEPO^{\bullet})$/$(py)_2Fe^{III}(OEPO)$ clearly show that methylene protons on a single pyrrole ring can experience opposite (that is both upfield and downfield) hyperfine shifts.[30]

The ability of axial ligation to effect the electronic distribution between the metal and the tetrapyrrole ligand as must occur in the interconversion of intermediates **4**, with a significant contribution from the $[ClFe^{II}(OEB^{\bullet})]^-$ form, and **3** is well precedented. Thus, addition of pyridine to $[Co^{II}(OEBOx)]I_3$, with an EPR spectrum characteristic of a Co(II) species with *g* tensor values of 2.42, 2.33, and 2.01 in frozen solution, produces $[(py)_2Co^{III}(OEB)]^+$ with an EPR spectrum that shows only a slightly anisotripic spectrum, with *g* values of 1.996 and 2.018.[31] The latter signal is assigned to a ligand-based radical complexed to Co(III). Similar behavior to that observed in the conversion of **4**−Cl to **5** is seen in the addition of methoxide ion to $(py)_nFe^{II}$(OEBOMe), as seen in Figures 7 and 8 and Scheme 4.[19] Here again, the new intermediate **6** displays an ^{1}H NMR spectrum with methylene resonances with both upfield and downfield hyperfine shifts that suggest significant contribution from a ligand radical component in the overall electronic structure. Our observations are consistent with a thesis that the presence of methoxide or hydroxide as axial ligand is necessary to generate the radical-like NMR spectrum from $(py)_nFe^{II}$(OEBOMe) and that the degree of the conversion depends on the anionic ligand choice.

In conclusion, an iron biliverdin radical species seems to be an essential intermediate in the process of iron octaethylporphyrin degradation (coupled oxidation). It remains to be seen if such radical species will be directly detected in the biochemical process. The paramagnetic shift patterns for the model iron OEB-related radical complexes present several useful and potentially unique probes for detecting the analogous species in hemoproteins by ^{1}H NMR spectroscopy.

Experimental Section

Preparation of Compounds. The iron complexes, $[(py)_2Fe^{II}(OEOP)]Cl$,[1] $Cl_2Fe^{III}(OEOP)$,[1] and $\{Fe^{II}(OEBOMe)\}_2$[19] were prepared as described previously.

Preparation of Meso-Deuterated Complexes. A 342.7 mg (0.611 mmol) sample of Mg^{II}(OEP-*meso*-d_4) was prepared via a known route[32] and transmetalated by reaction with $Fe^{II}Cl_2 \cdot 4H_2O$ to produce $ClFe^{III}$(OEP-*meso*-d_4). Subsequently, $ClFe^{III}$(OEP-*meso*-d_4) was converted into Cl_2Fe^{III}(OEOP-*meso*-d_3) by coupled oxidation in dichloromethane/pyridine with ascorbic acid as reductant, as described earlier,[1] with a yield of 131 mg (33%).

Hydroxide Addition to Cl_2Fe^{III}(OEOP). A 40 wt % solution of KOD in D_2O (Aldrich) was diluted with D_2O (1/9 v/v) to give an approximately 1.0 M solution. Alternatively, 400 mg of KOH was dissolved in 0.54 mL of D_2O (to give a 40% solution) and then diluted with D_2O as previously described, but in this case the residual HOD signal was considerably stronger. Titrations with these hydroxide solutions into septum sealed NMR tubes (to avoid additional D − H exchange) were performed with a 10 μL syringe. The sample concentration for the iron complexes in the solvent of choice (chloroform-*d*, dichloromethane-d_2, DMSO-d_6, or acetonitrile-d_3) were on the order of 1−3 mM and typically required 2−20 μL of the hydroxide solution to be added to 0.45 mL of the solution of the verdoheme for complete conversion. Visual inspection suggests that this produces a homogeneous sample, and the ^{1}H NMR spectra of such samples do not show a separate HDO resonance from a second phase. In the initial stage of experiments, the samples of Cl_2Fe^{III}(OEOP) were prepared and sealed in dioxygen free solvents under dinitrogen atmosphere in a glovebox. However, it has been shown that the results of titration did not depend on the presence of dioxygen. Consequently, all subsequent measurements were carried out in the presence of dioxygen.

Methoxide and Hydroxide Addition to $\{Fe^{II}$(OEBOMe)$\}_2$. Samples were prepared by dissolving $\{Fe^{II}(OEBOMe)\}_2$ in pyridine-d_5. All samples and titrating solutions were prepared and sealed in dioxygen free solvents under the dinitrogen atmosphere in a glovebox. A solution of sodium methoxide-d_3 was prepared by dissolution of 100 μL of 40 wt % KOD/D_2O in 2 mL of methanol-d_4. Alternatively, 100 mg of KOH were dissolved in 3 mL of methanol-d_4. Reactions with either methoxide source produced similar results. Titrations of methoxide-d_3 solutions into septum sealed NMR tubes were performed with 10 mL syringes. Sample concentration for the iron complexes in pyridine-d_5 were in the range of 1−3 mM. Potassium hydroxide solutions in D_2O were prepared as described above for the verdoheme titration.

Instrumentation. ^{1}H NMR spectra were recorded on a General Electric QE−300 FT NMR spectrometer, a Bruker AMX300 Spectrometer, or a Bruker Avance 500 Spectrometer operating in the quadrature mode (^{1}H frequency is 300 MHz for the first two spectrometers and 500 MHz for the last). An exponential window function was applied to improve the signal-to-noise ratio. The residual ^{1}H resonances of the deuterated solvents were used as secondary references.

Abbreviations used: (OEP), dianion of octaethylporphyrin; (OEOP), anion of octaethyl-5-oxaporphyrin; (OEB), trianion of octaethylbilindione; (OEBOMe), dianion of octaethylmethoxybiliverdin; py, pyridine.

Acknowledgment. We thank the NIH (GM-26226) (to A.L.B.) and the Foundation for Polish Science (to L.L.G., J.W.) for financial support and Dr. Nasser Safari for key assistance in the initial stages of this project.

IC010227A

(27) Lord, P. A.; Olmstead, M. M.; Balch, A. L. *Inorg. Chem*. **2000**, *39*, 1128.
(28) Morishima, I.; Shiro, Y.; Wakino, T. *J. Am. Chem. Soc*. **1985**, *107*, 1063.
(29) Balch, A. L.; Koerner, R.; Latos-Grażyński, L.; Noll, B. C. *J. Am. Chem. Soc*. **1996**, *118*, 2760.
(30) Kalish, H. R.; Latos-Grażyński, L.; Balch, A. L. *J. Am. Chem. Soc*. **2000**, *122*, 12478.
(31) Attar, S.; Ozarowski, A.; Van Calcar, P. M.; Winkler, K.; Balch, A. L. *Chem. Commun*. **1997**, 1115.
(32) Bonnett, R.; Gale, I. A. D.; Stephenson, G. F. *J. Chem. Soc. C* **1967**, 1169.